ALMA Memo No. 558
Thermal Deformation of Shaped Carbon Fiber-Aluminum Core Sandwiched Structures(II)

Jingquan Cheng
NRAO, Oct. 2006
jcheng@nrao.edu

ROAD MAP
FOR MEMOS 557,558, and 559

Early in 2000, one type of ALMA antenna BUS design was proposed which involved a channel shaped carbon fiber aluminum honeycore sandwiched structure. This type of structure will change its shape as the temperature changes. For verifying this thermal shape change problem, three internal memos were produced in Aug. 2000. These were reproduced here as ALMA Memo Nos. 557, 558 and 559. Memo No. 557 is the first memo which provides theoretical derivation as well as a simple finite element analysis. The memo pointed out that if the channel width is 1m, the surface deformation will be 33 um. The FEA analysis uses a coarse element size. Memo No. 558 is a refined analysis with different constraint conditions. The analysis results are consistent with the first memo. Memo No. 559 is a detailed analysis of the corner problem area. This corner area has high stress concentration, complex strain, and is the main reason for the shape change of the top surface.

In Sept, 2001, a BUS section was tested to verify its thermal performance. After the test data were processed, an internal report was produced. The title of the report is: Antenna BUS Thermal Test Evaluation Report. In this report, test data were used to check the predictions of the early memos. An estimation of the antenna surface deformation was also made from the measurement. If the early BUS design was used, the surface rms error could reach 28 um. The report also provided the explanation of the adjuster's preload change as temperature changes. The internal stress level between the BUS and the panels were also estimated. The highest internal force between panel and BUS may reach 50,000N when temperature change is large.

After these analyses, the sandwiched BUS structure design was modified. In the modified design, the stress of the corner part is absorbed. The top surface has little thermal deformation. These modified ALMA BUS structures were also applied to APEX and the South Pole Sub-millimeter Telescope. As these memos and this report played an important role in ALMA antenna design, these memos are reproduced as they were. The report remains out of public domain. However, astronomers could request the report with conditions.

Thermal Deformation of Shaped Carbon Fiber-Aluminium Core Sandwiched Structures(II)

Jingquan Cheng
National Radio Astronomy Observatory

August, 2000

Abstract

Thermal deformation of T-shaped, L-shaped and channel shaped structures are discussed in the previous report. The work here shows that the computer analysis with smaller element size is consistant with the prediction. It also shows that over-constraint usually produces larger thermal deforamtion.

1 Introduction

In the previous report(Thermal Deformation of Shaped Carbon Fiber- Aluminium Core Sandwiched Structures, by Jingquan Cheng), the basic deformation patterns of the top plate of a T-shaped, an L-shaped, and a channel shaped structure are discussed when the vertical plate is constrained. The analysis method is simple and the finite element model is coarse. For further understanding the deformation of a channel shaped structure and the effects of constraints, a refined model is made and analysis is done when different constraints are applied. This report is a supplement of the previous report.

2 Computer analysis with models of a smaller element size

In the previous report the element size in the computer analysis is larger. Therefore, a number of body force effects when the temperature changes have been neglected. The resulted deformation pattern will hide a number of details. For this reason a new model is made as show in Figure 1. In this model, the sandwich core is represented by two layers of elements instead of only one layer in the previous model. This results an eight times increase in element numbers. The section model is still a part of a slice of a pie-shaped channel. It has an extended angle of 15 degrees. The channel section inner edge to the pie center is 3 m and the outer edge to the pie center is 3.5 m. The channel width of the inner side is therefore D=0.78 m and the outer side is D=0.91 m. The thickness of the top plate is h=0.072 m and that for the vertical plates is d=0.02 m. In the analysis, the skin thickness used is 0.0005 m. The modulus of CFRP skin is E=190 GPa and that for the aluminum core is 270 MPa. The density of CFRP is 2150 kg/m^3 and that for the core is 83 kg/m^3. The temperature increase is 20 degrees C. The structural constraint is also shown in Figure 1. It is a constraint of both vertical plates. The constraint grids is near the top surface. Figures 2 and 3 are top and bottom deformation patterns of this case. From these two figures, the maximum deformations of the top surface is 69 μm, a 10 μm smaller than the coarse model result. The same as the bottom deformation, the maximum for the bottom surface is only 10 μm. However, the bottom surface has a region with negative deformation. The minimum is a little less than -10 μm. Adding this negative number, the deformation numbers agree with the coarse model results. The negative results may partly be caused by the model itself. The new model bottom surface is not on a perfect plane. The patterns on both surfaces have edge and constraint effects. These effects are not shown in the results of the previous model.

3 Computer analysis with models of different constraints

We also applied various constraints on the structure. The patterns are produced for a number of different constraint cases. Figures 4 and 5 are patterns of 16 grids constraint. The constrained grids are shown in the figures. The deformation patterns shown are larger than those in Figures 2 and 3. This is the result of an over constraint.

Figures 6 and 7 are patterns for 10 positions, 18 grids constraint case. The additional two constrained grids are on the bottom side of the top plate. Because the additional supports is not in the center of bottom side, that does not help in reducing structure deformation.

Figures 9 and 10 are patterns for the case of 19 grids constraint case. The added new grid is in the center of the bottom surface of the top plate.

The new constrant reduces the deformations on both top and bottom sides. The bottom side is much smoother.

Figures 10 and 11 are the case of which three more girds are added on the other edge of the bottom side of the top plate. The patterns show that this addition does not help in reducing the structure deformation.

In the analysis, we used a real CTEs for CFRP plate($0.6X10^{-6\o}C^{-1}$) and for aluminum($24X10^{-6\o}C^{-1}$). We also run the analysis by using a zero CTE for CFRP plate and a reduced CTE for aluminum($23X10^{-6\o}C^{-1}$), the patterns produced are similar. The resulted deformations are slightly smaller for the later CTE assumption.

4 Conclusion

Based on the balance of the internal forces, the analysis results with finer elements agrees with theoretical prediction as well as the coarse element model analysis. With a vertical plate constraint, the deformation of a channel shaped sandwich structure is complex and serious. However, thermal expansion of laminated or sandwich honeycomb structures may not follow exactly the role of finite element theory. These structures are not isotropic in property and they involve other internal forces. For example the bond surface forces between plate and core and the friction forces between fibers and matrix are both not easy to model and their effects are not included in the finite element theory. For this reason, the above calculation and prediction can only be used as a gerenal reference. The best way to assess this complex problem is to produce a real structure and to take a direct measurement. However, the measurement itself is also difficult. We have to be careful to avoid the thermal errors of the measuring device. These errors may have the same magnitude of the deformation.

5 Figures

Figure 1 Finite element model of a channel sandwich structure with a smaller element size.

Figure 2 Deformation pattern of 8 grids constraint when temperature increases 20 degrees C.

Figure 3 Deformation pattern of 8 grids constraint when temperature increases 20 degrees C(bottom view).

Figure 4 Deformation pattern of 16 grids constraint when temperature increases 20 degrees C.

Figure 5 Deformation pattern of 16 grids constraint when temperature increases 20 degrees C(bottom view).

Figure 6 Deformation pattern of 18 grids constraint when temperature increases 20 degrees C.

Figure 7 Deformation pattern of 18 grids constraint when temperature increases 20 degrees C(bottom view).

Figure 8 Deformation pattern of 19 grids constraint when temperature increases 20 degrees C.

Figure 9 Deformation pattern of 19 grids constraint when temperature increases 20 degrees C(bottom view).

Figure 10 Deformation pattern of 22 grids constraint when temperature increases 20 degrees C.

Figure 11 Deformation pattern of 22 grids constraint when temperature increases 20 degrees C(bottom view).

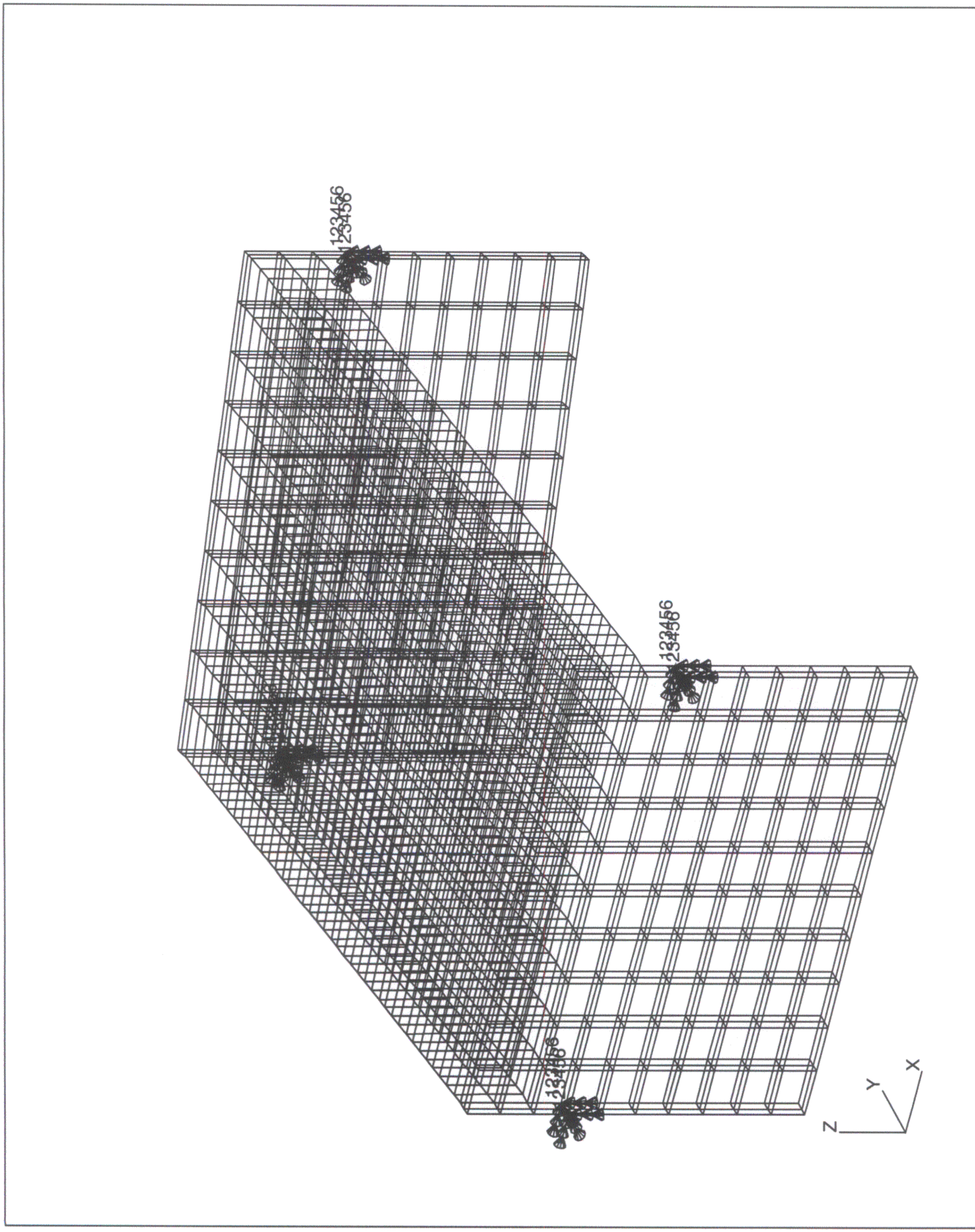

FIGURE 1

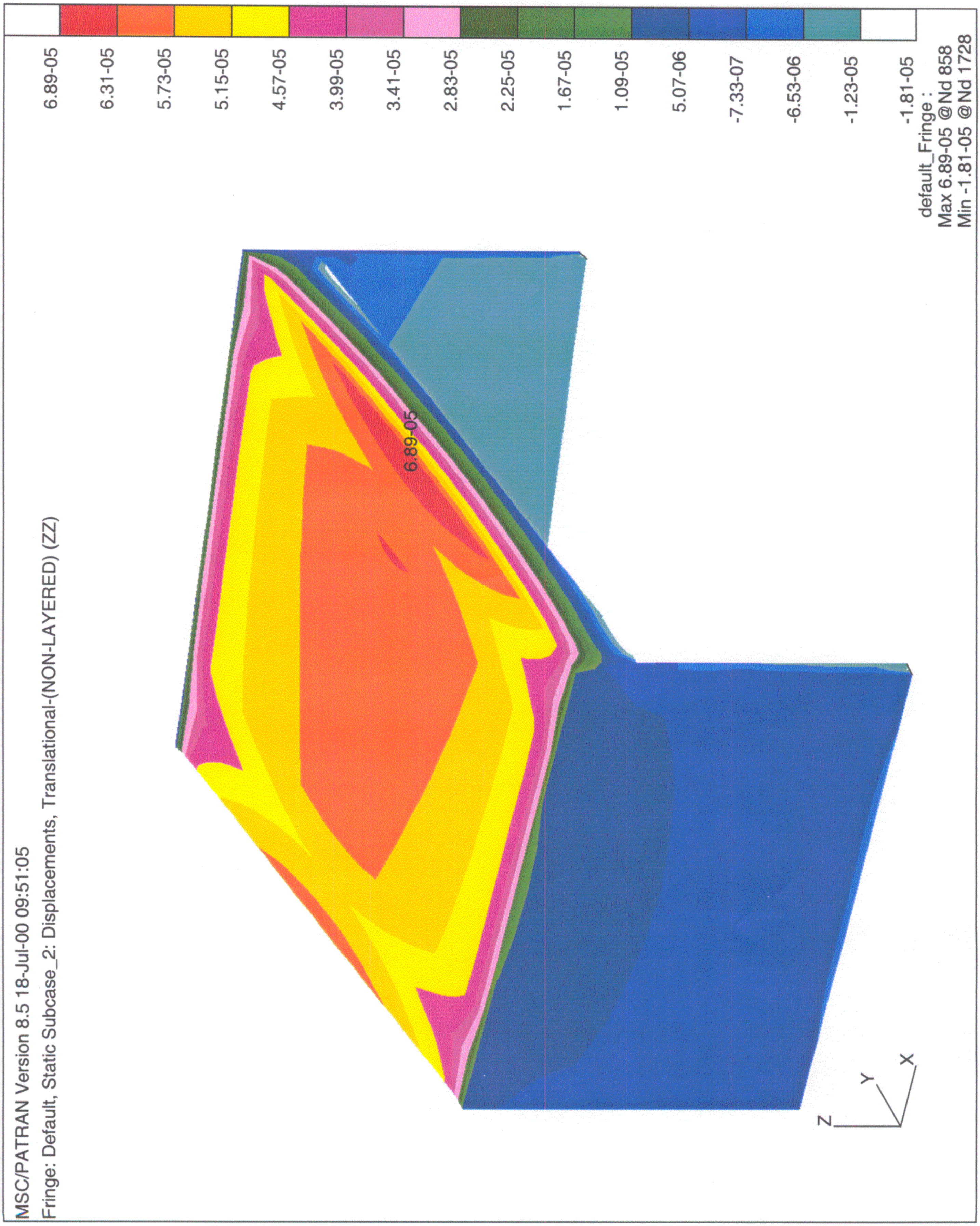
MSC/PATRAN Version 8.5 18-Jul-00 09:51:05
Fringe: Default, Static Subcase_2: Displacements, Translational-(NON-LAYERED) (ZZ)
6.89-05
6.31-05
5.73-05
5.15-05
4.57-05
3.99-05
3.41-05
2.83-05
2.25-05
1.67-05
1.09-05
5.07-06
-7.33-07
-6.53-06
-1.23-05
-1.81-05
default_Fringe :
Max 6.89-05 @Nd 858
Min -1.81-05 @Nd 1728
6.89-05
Z
Y
X

FIGURE 2

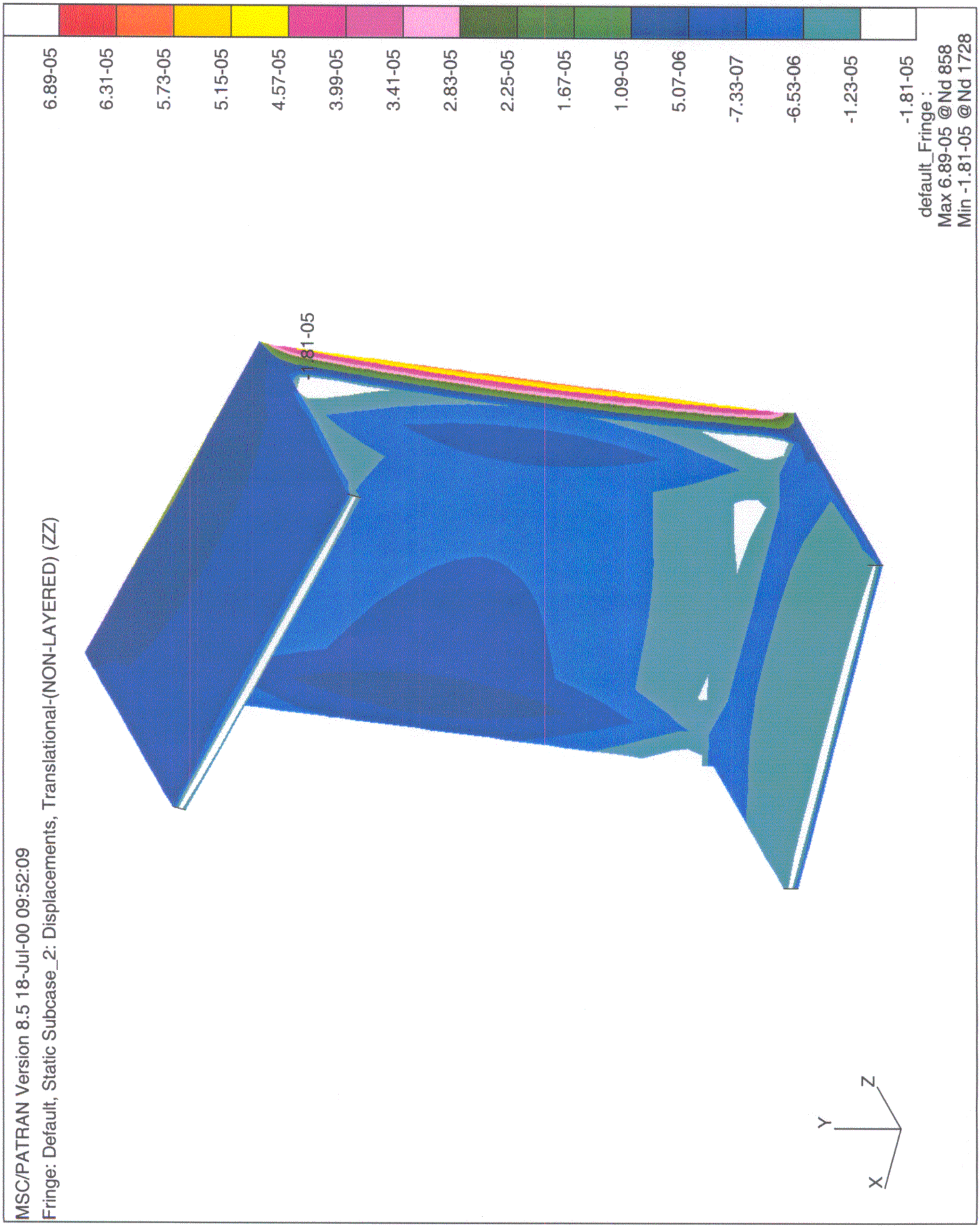
MSC/PATRAN Version 8.5 18-Jul-00 09:52:09
Fringe: Default, Static Subcase_2: Displacements, Translational-(NON-LAYERED) (ZZ)
6.89-05
6.31-05
5.73-05
5.15-05
4.57-05
3.99-05
3.41-05
2.83-05
2.25-05
1.67-05
1.09-05
5.07-06
-7.33-07
-6.53-06
-1.23-05
-1.81-05
default_Fringe :
Max 6.89-05 @Nd 858
Min -1.81-05 @Nd 1728
-1.81-05
X
Y
Z

FIGURE 3


MSC/PATRAN Version 8.5 19-Jul-00 08:46:50
Fringe: Default, Static Subcase: Displacements, Translational-(NON-LAYERED) (ZZ)
7.86-05
7.24-05
6.62-05
6.00-05
5.38-05
4.76-05
4.14-05
3.52-05
2.90-05
2.28-05
1.66-05
1.04-05
4.23-06
-1.97-06
-8.17-06
-1.44-05
default_Fringe :
Max 7.86-05 @Nd 858
Min -1.44-05 @Nd 1728
Z
Y
X

FIGURE 4

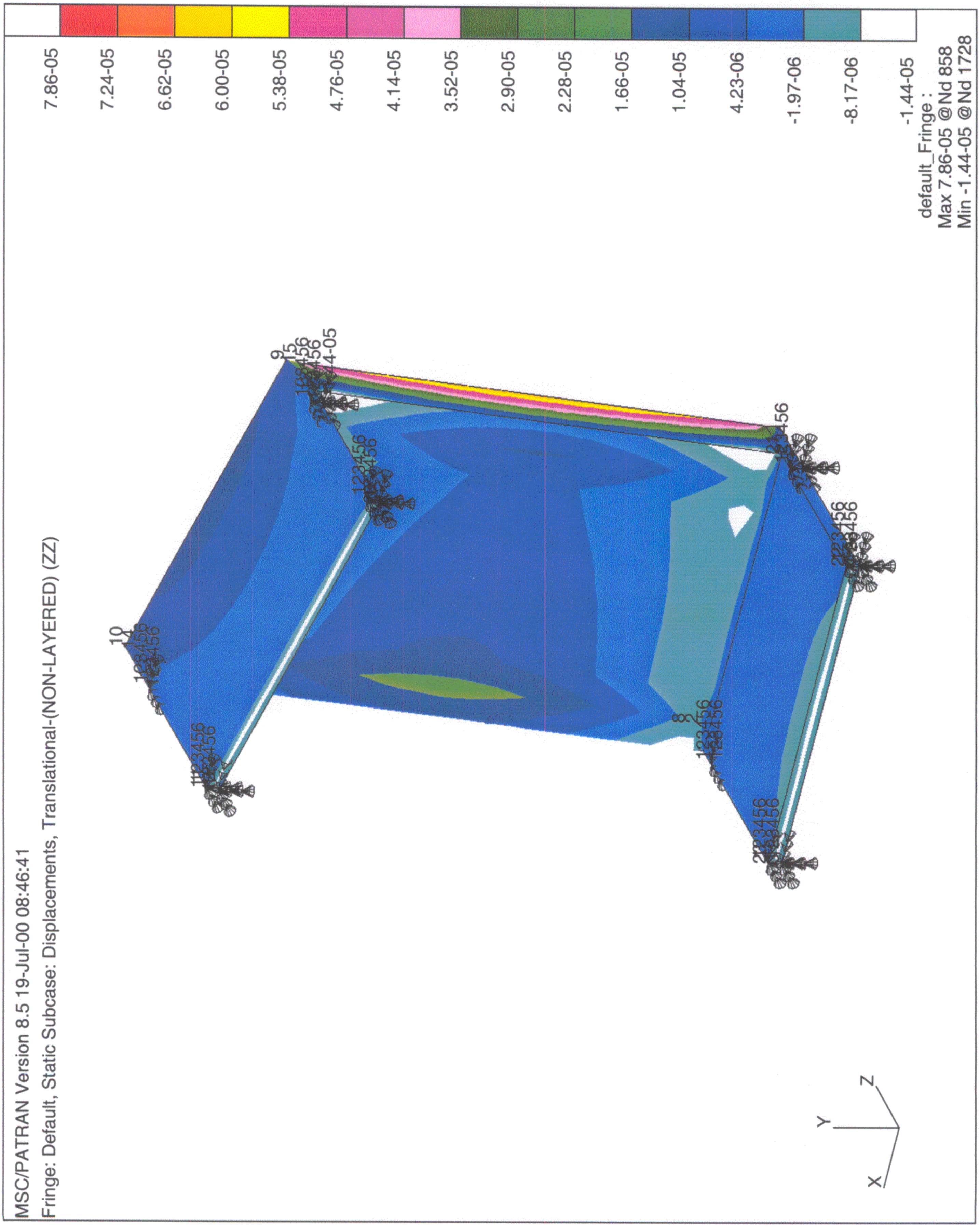
MSC/PATRAN Version 8.5 19-Jul-00 08:46:41
Fringe: Default, Static Subcase: Displacements, Translational-(NON-LAYERED) (ZZ)
7.86-05
7.24-05
6.62-05
6.00-05
5.38-05
4.76-05
4.14-05
3.52-05
2.90-05
2.28-05
1.66-05
1.04-05
4.23-06
-1.97-06
-8.17-06
-1.44-05
default_Fringe :
Max 7.86-05 @Nd 858
Min -1.44-05 @Nd 1728
X
Y
Z

FIGURE 5

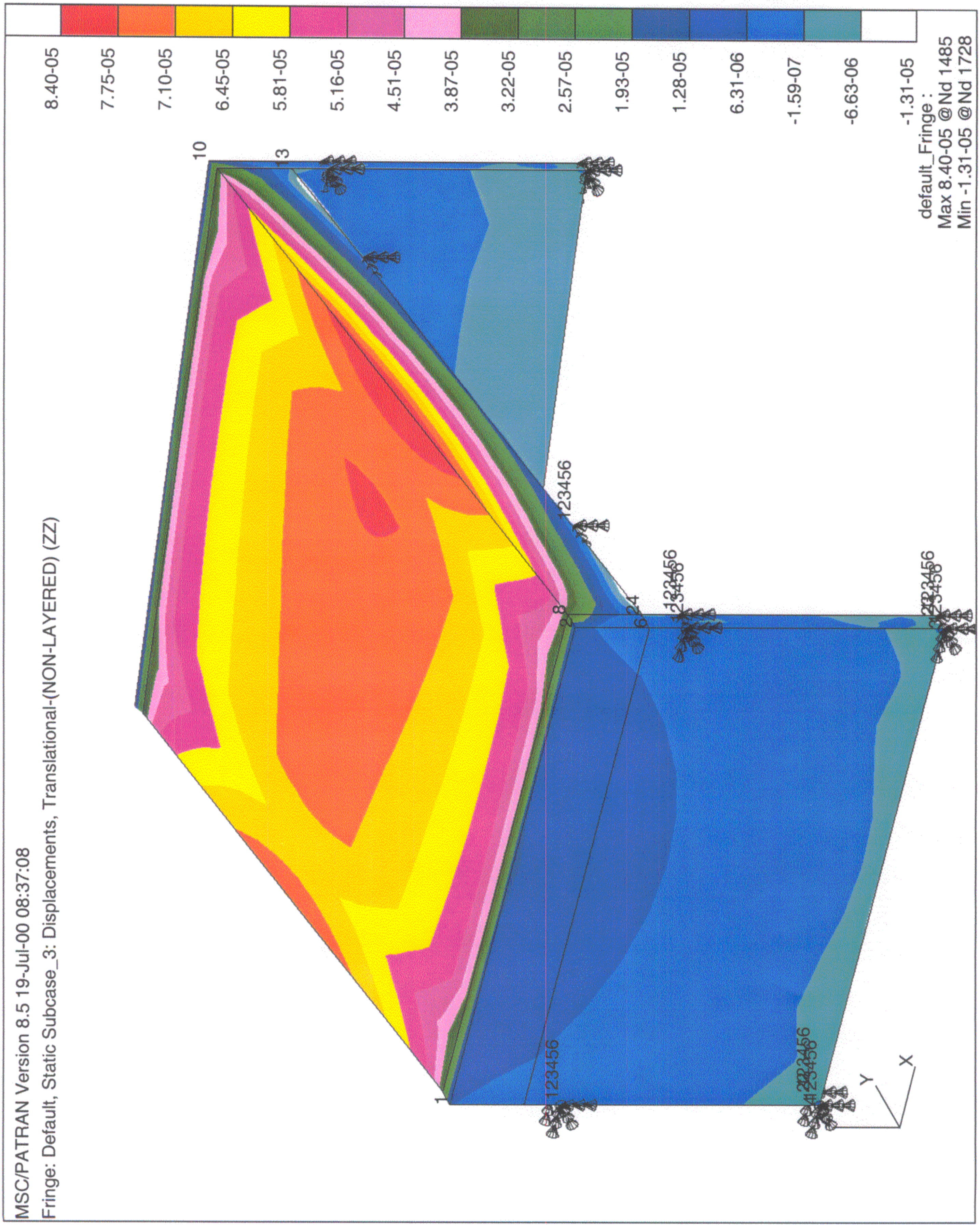
MSC/PATRAN Version 8.5 19-Jul-00 08:37:08
Fringe: Default, Static Subcase_3: Displacements, Translational-(NON-LAYERED) (ZZ)
8.40-05
7.75-05
7.10-05
6.45-05
5.81-05
5.16-05
4.51-05
3.87-05
3.22-05
2.57-05
1.93-05
1.28-05
6.31-06
-1.59-07
-6.63-06
-1.31-05
default_Fringe :
Max 8.40-05 @Nd 1485
Min -1.31-05 @Nd 1728
Y
X

FIGURE 6

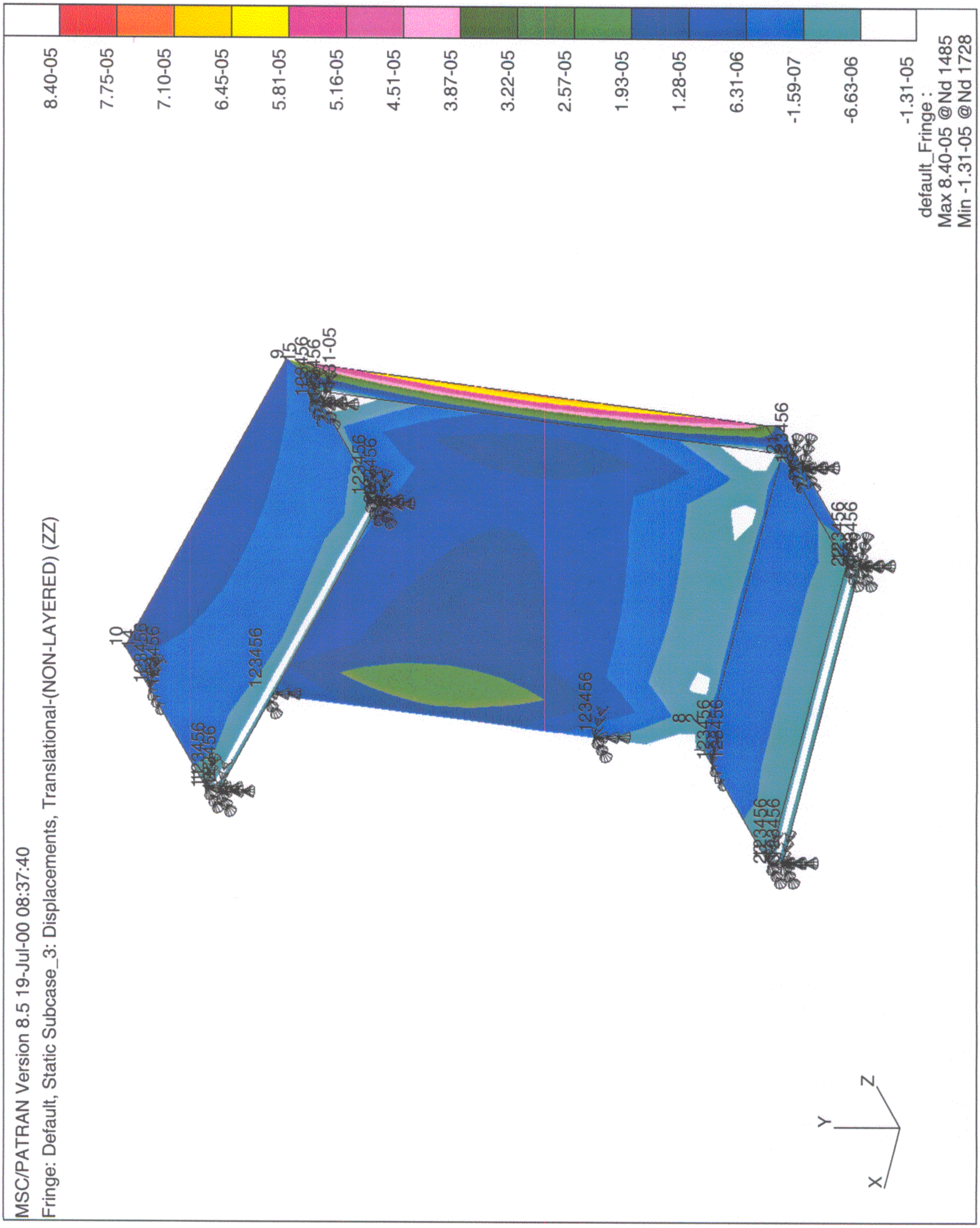
MSC/PATRAN Version 8.5 19-Jul-00 08:37:40
Fringe: Default, Static Subcase_3: Displacements, Translational-(NON-LAYERED) (ZZ)
8.40-05
7.75-05
7.10-05
6.45-05
5.81-05
5.16-05
4.51-05
3.87-05
3.22-05
2.57-05
1.93-05
1.28-05
6.31-06
-1.59-07
-6.63-06
-1.31-05
default_Fringe :
Max 8.40-05 @Nd 1485
Min -1.31-05 @Nd 1728
X
Y
Z

FIGURE 7

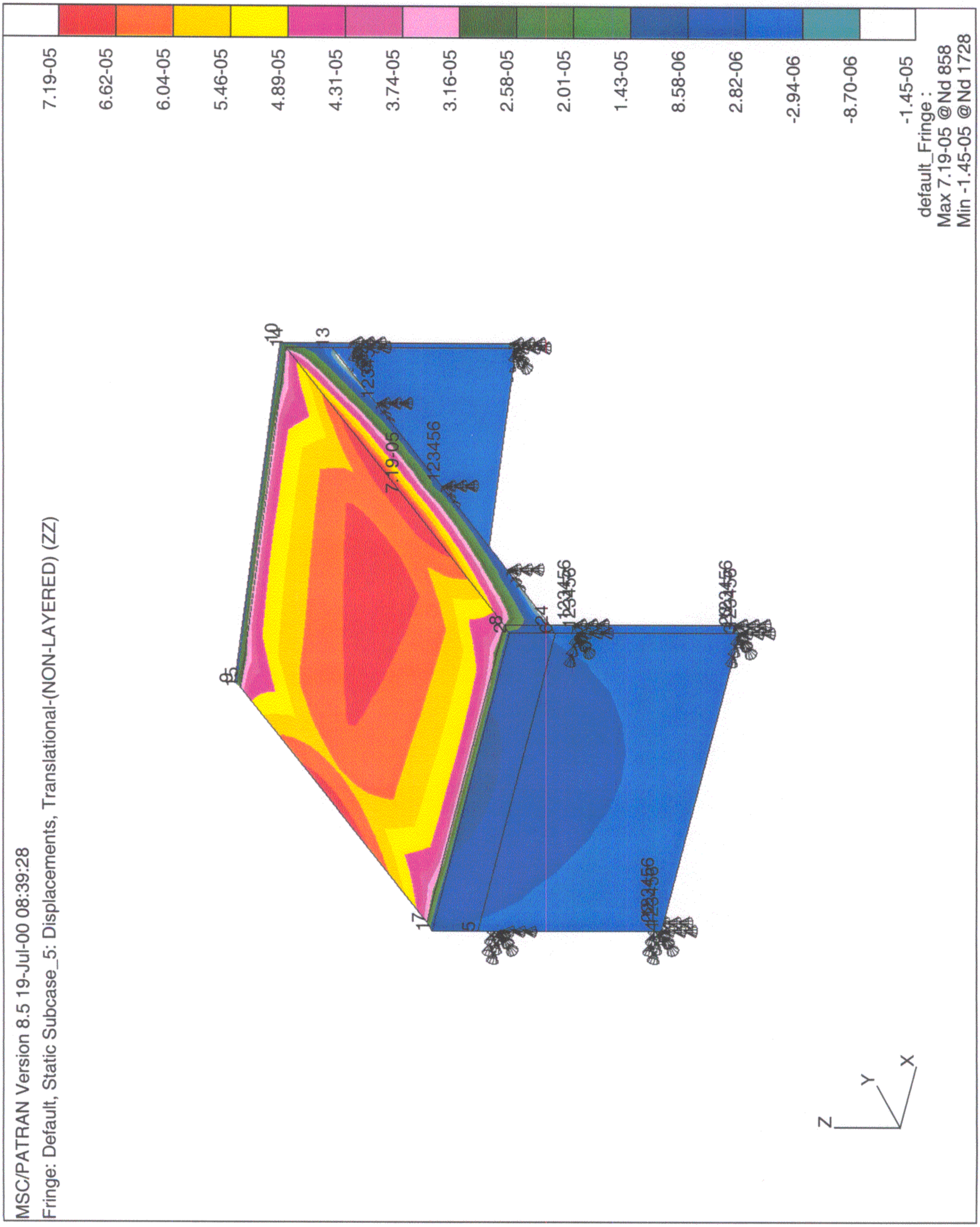

MSC/PATRAN Version 8.5 19-Jul-00 08:39:28
Fringe: Default, Static Subcase_5: Displacements, Translational-(NON-LAYERED) (ZZ)
7.19-05
6.62-05
6.04-05
5.46-05
4.89-05
4.31-05
3.74-05
3.16-05
2.58-05
2.01-05
1.43-05
8.58-06
2.82-06
-2.94-06
-8.70-06
-1.45-05
default_Fringe :
Max 7.19-05 @Nd 858
Min -1.45-05 @Nd 1728
7.19-05
123456
Z
Y
X

FIGURE 8

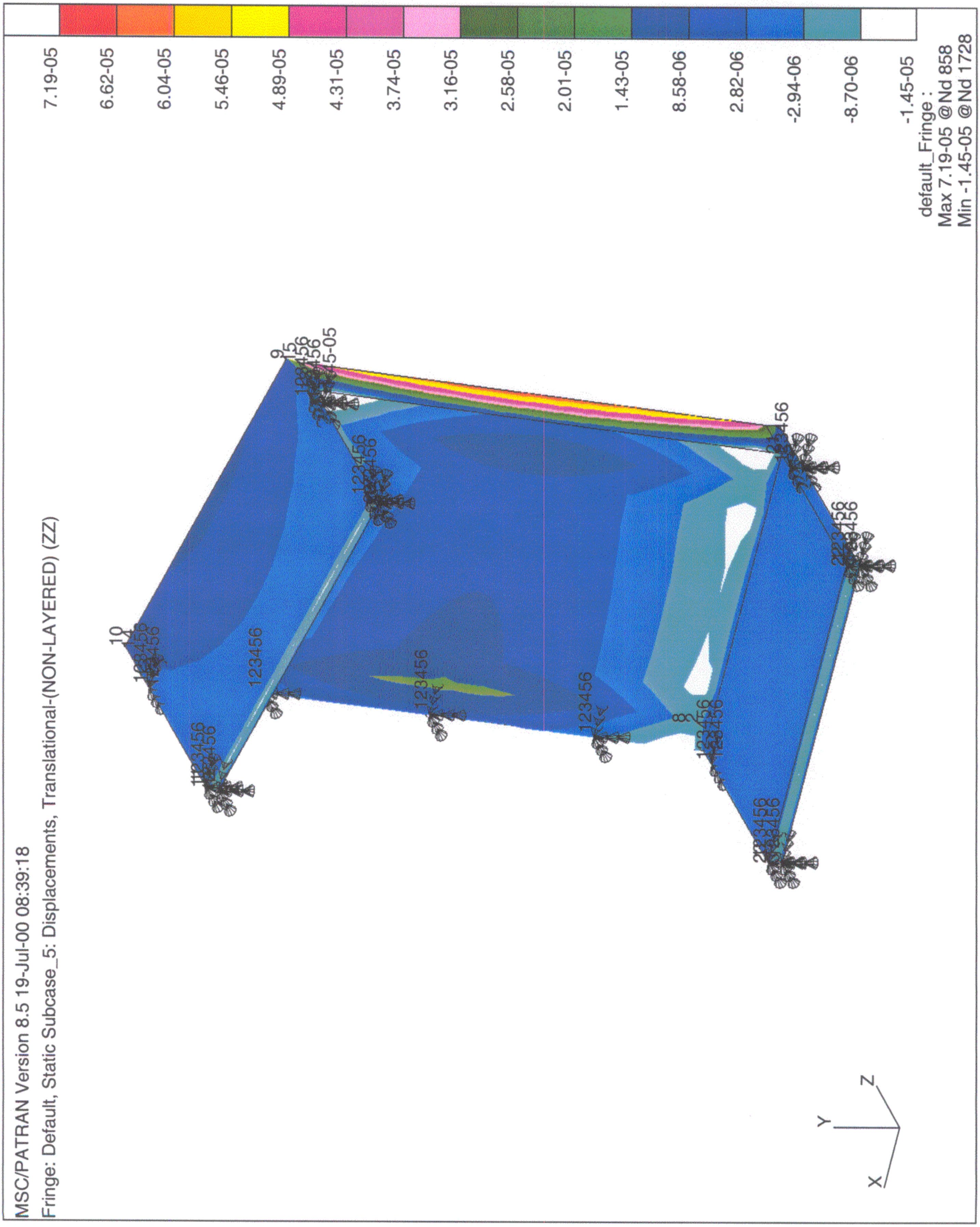

MSC/PATRAN Version 8.5 19-Jul-00 08:39:18
Fringe: Default, Static Subcase_5: Displacements, Translational-(NON-LAYERED) (ZZ)
7.19-05
6.62-05
6.04-05
5.46-05
4.89-05
4.31-05
3.74-05
3.16-05
2.58-05
2.01-05
1.43-05
8.58-06
2.82-06
-2.94-06
-8.70-06
-1.45-05
default_Fringe :
Max 7.19-05 @Nd 858
Min -1.45-05 @Nd 1728
123456
X
Y
Z

FIGURE 9

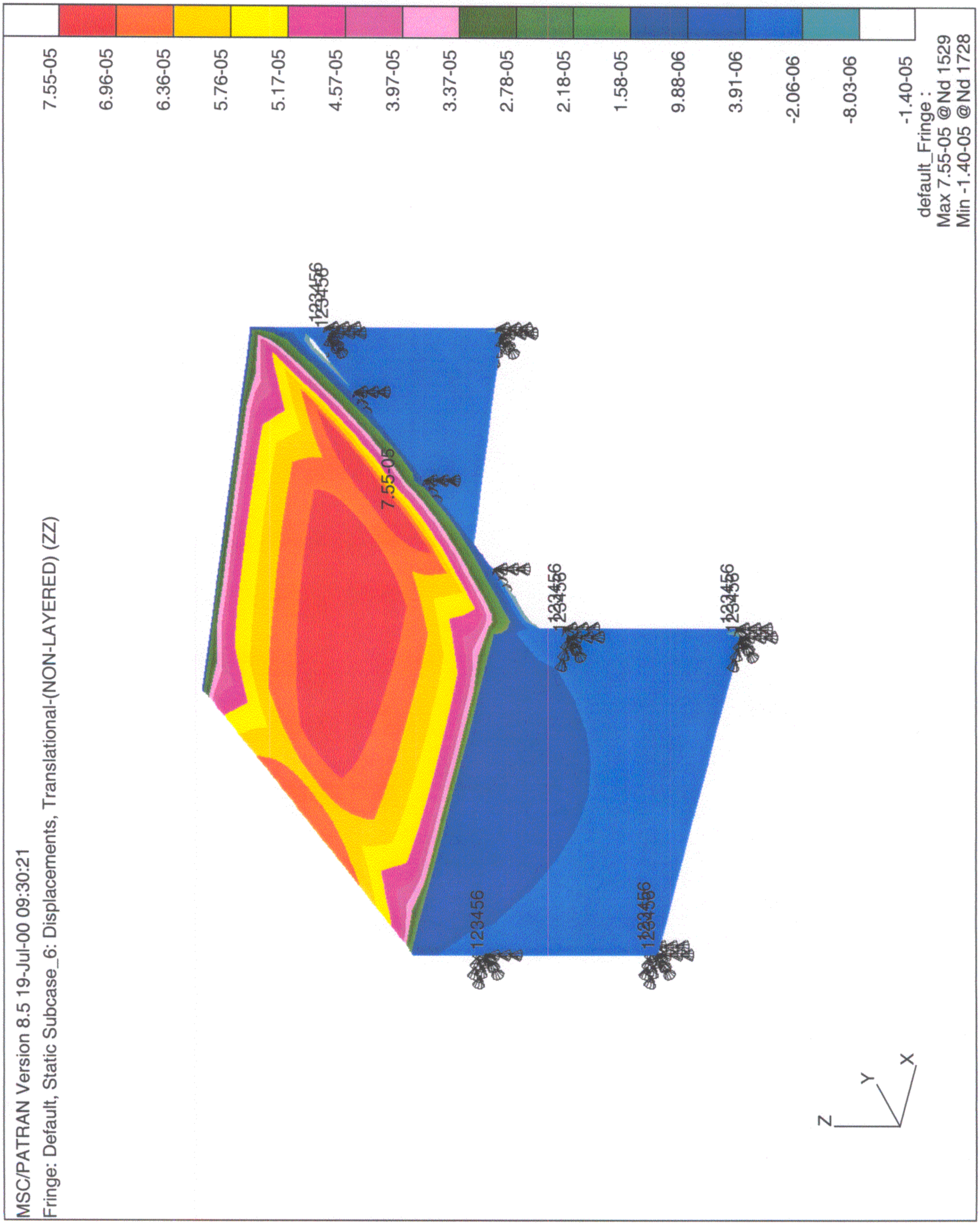
MSC/PATRAN Version 8.5 19-Jul-00 09:30:21
Fringe: Default, Static Subcase_6: Displacements, Translational-(NON-LAYERED) (ZZ)
7.55-05
6.96-05
6.36-05
5.76-05
5.17-05
4.57-05
3.97-05
3.37-05
2.78-05
2.18-05
1.58-05
9.88-06
3.91-06
-2.06-06
-8.03-06
-1.40-05
default_Fringe :
Max 7.55-05 @Nd 1529
Min -1.40-05 @Nd 1728
123456
7.55-05
Z
Y
X

FIGURE 10


MSC/PATRAN Version 8.5 19-Jul-00 09:29:48
Fringe: Default, Static Subcase_6: Displacements, Translational-(NON-LAYERED) (ZZ)
7.55-05
6.96-05
6.36-05
5.76-05
5.17-05
4.57-05
3.97-05
3.37-05
2.78-05
2.18-05
1.58-05
9.88-06
3.91-06
-2.06-06
-8.03-06
-1.40-05
default_Fringe :
Max 7.55-05 @Nd 1529
Min -1.40-05 @Nd 1728
X
Y
Z

FIGURE 11